Novel Insights into Membrane Transport from Computational Methodologies

Victoria Oakes[1] and Carmen Domene[1,2]

[1]*Department of Chemistry, Britannia House, 7 Trinity Street, King's College London, London SE1 1DB, U.K.*

[2]*Chemistry Research Laboratory, Mansfield Road, University of Oxford, Oxford OX1 3TA, U.K.*

Abstract

Atomic-resolution imaging of the plasma membrane and its constituents has advanced significantly in recent years. However, membrane transport is profoundly reliant on dynamic processes ranging from highly concerted atomic fluctuations to large-scale conformational changes, which cannot be sufficiently described by static structural information. As a consequence, computational methodologies have become a prominent tool to investigate membrane organisation and dynamics. In particular, molecular dynamics simulation has proven to be a pertinent method to investigate how matter is transported through membranes, either directly through the membrane or via integral membrane proteins, in an appropriate level of detail. In this chapter, we will provide a brief overview of molecular dynamics simulations and related methodologies, and use prototypical biological systems to illustrate how these methods have contributed to our understanding of unassisted diffusion through membranes, passive diffusion through ion channels, signalling through receptors and active transport through transporters.

Introduction

The plasma membrane is an integral constituent of both prokaryotic and eukaryotic cells, enclosing the cytoplasm and other cell components. In the latter, the biological membrane is the primary instrument governing the passage of solutes to the cell interior. A phospholipid bilayer forms the basic structural unit establishing a hydrophobic barrier in the membrane core, thus whilst hydrophobic molecules may be admitted passage, additional biological assemblies are required for the transmission of many molecules. Membrane proteins, as these assemblies are known, also play a role in cell signalling, invoking internal processes on recognition of external stimuli. A schematic of membrane transport phenomenon can be found in Figure 1.

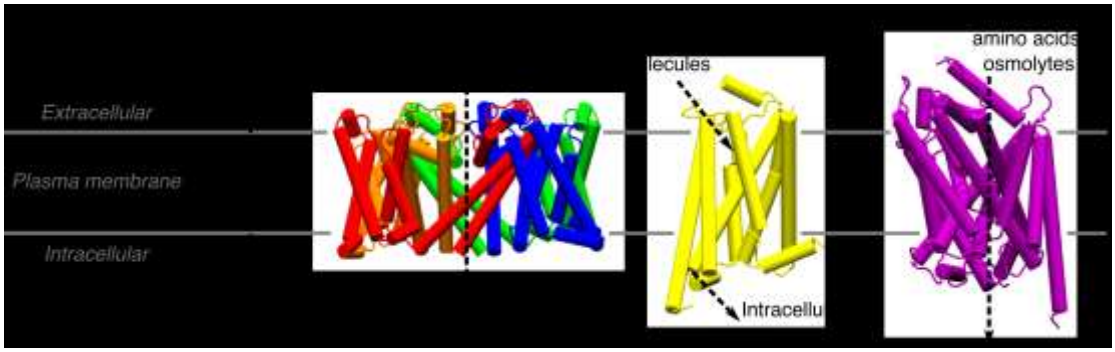

Figure 1. Schematic of transport phenomenon across the plasma membrane: hydrophobic drug molecules transit directly through the lipid membrane; ions passively diffuse down the electrochemical gradient of the membrane via ion channels, represented as the Na_VAb sodium voltage-gated channel (individual subunits coloured blue, red, yellow and green); binding of extracellular molecules to G-protein coupled receptors initiates coupling with intracellular partners and subsequent signalling, represented as the β2-adrenergic receptor (yellow); molecules can also be actively transported across the membrane, such as amino acids through Na^+-coupled secondary symporters, represented as the leucine transporter (purple).

The availability of atomic resolution structural information is pivotal to discern the underlying principles of membrane transport and communication phenomenon. Vast developments in X-ray crystallographic techniques, NMR and innovative structural

determination methods, such as electron cryo-microscopy, have revolutionized our understanding of the three-dimensional structure of membrane proteins.[1] In combination with the current availability of state-of-the-art computational algorithms and high-performance computing facilities, molecular dynamics (MD) simulations of membrane proteins in a model environment can now be performed routinely to explore a wide range of biological phenomena providing insight for which no experimental methods are applicable. Exploration of the dynamic behaviour of such entities in atomic detail has become particularly important in the realm of medicinal chemistry, where familiarity of ligand transport and binding processes, and subsequent activation or deactivation mechanisms, can lead to the rational design of drugs with improved potency and efficacy, reduced toxicity and subtype specificity. In the following text, we aim to review the considerable insights gained from computational methodologies in recent years.

Computational Methods

A wide variety of computational methods are currently applied in the field of computational chemistry. MD is a common method used to obtain time-dependent behaviour of a chemical system. In this method, the motion of interacting particles is calculated by the integration of Newton's equations of motion (EOM). The potential energy of the system and the forces, derived from the negative gradient of the potential with respect to displacement in a specified direction, can be used to calculate the acceleration, and hence forecast the time evolution of the system, in the form of a trajectory.

In systems with a couple of atoms, solutions of EOM can be gained analytically, resulting in a continuous trajectory over time. However, in larger systems, the subsistence of a continuous potential instigates a many body problem for force evaluations, rendering analytic solutions unattainable. In these circumstances, finite difference methods can be used; forces are assessed at discrete intervals, and considered constant in the hiatus. Positions and velocities at the next timestep, as these intervals are known, are computed using force evaluations for each atom combined with current positions and velocities. Forces are then recalculated and this procedure is repeated, propagating a trajectory describing the flux of the atomic

coordinates over time in a given equilibrium state, which can then be analysed for the properties of interest.

The potential energy can be obtained by quantum or molecular mechanical methods. In the former, only the nuclear motion is evaluated using classical physics; atoms and bonds are considered as balls and springs, respectively, and an analytical expression for the energy of a system, known as a forcefield, can be derived. This is composed entirely of inter- and intramolecular energetic contributions, including bond stretching, angle bending, bond rotations and non-bonded terms. This architecture neglects electronic properties, such as dipole moments, polarisabilities and vibrational frequencies, but allows for the evaluation of molecular motion for (biological) systems with a large number of degrees of freedom predominant due to reduced computational expense. A wide variety of forcefields for biological molecules are available including, but not limited to CHARMM (Chemistry at Harvard Molecular Mechanics),[2] AMBER (Assisted Model Building with Energy Requirement),[3] and OPLS (Optimized Potentials for Liquid Simulations).[4] Each varies in their functional form, parameterisation protocol and parameters therein, which are generally obtained to provide a suitable reproduction of experimental and/or quantum mechanical data.

Most commonly, individual terms for bond lengths and angles utilise simple harmonic potentials on the basis of an energetic penalty associated with a deviation from the equilibrium value.[2] A torsional angle potential function is also typical to model steric barriers associated with the rotation of atoms. With respect to non-bonded interactions, Coulomb and Lennard-Jones potentials are used to express electrostatic and van der Waals forces respectively. In order to appertain electrostatic forces via the Coulomb formula, fixed-point charges are assigned at the nuclei. However, in reality, molecules are subject to polarisation effects, i.e. the charge fluctuates response to an external electric field, induced by the presence of additional molecules, thus highlighting a limitation of additive forcefields.[5]

Significant efforts to develop polarisable FF have been undertaken in recent years. Several schemes have been proposed, among which are the fluctuating charge model, the induced dipole model and the Drude oscillator approach. In the

fluctuating charge model, adopted in in the CHeq forcefield[6-7] for example, molecular charges remain constant throughout the simulation with individual point charges readjusted in consonance with the electronegativity. AMOEBA is the most noteworthy forcefield utilising an induced dipole model, where atomic multipoles are used explicitly to represent electrostatics; multipoles are calculated via a self-consistent field procedure, heightening the computational expense of this protocol.[8] Finally, in the Drude oscillator approach, a subsidiary charged particle is attached to the nucleus by a harmonic spring, and treated as an extra degree of freedom.[9] A comprehensive review of the field can be found in reference [10].[10]

Despite the universal availability of MD algorithms and forcefields applicable to biological macromolecules, the size of model systems of intrinsic membrane proteins, and the computing resources this requires, poses inherent limitations. The timestep suitable for stable dynamics is dictated by the highest vibrational frequency of the molecule, usually the C-H bond; 1 fs is commonplace, with 2 fs permitted when supplementary algorithms such as SETTLE,[11] an analytical version of the SHAKE function are employed to the movement of these bonds. In combination with system size up to 1,000,000 atoms, dynamics can be extremely intensive.[12] Recent expansions in computer hardware and high-performance computing facilities, means MD simulations on a nanosecond timescale are now routine, with microsecond simulations attainable in recent years. Such methodologies are therefore relevant to study a wide range of biological phenomena. Many biological phenomena that occur on extended timescales, such as protein folding, complex association and conformational changes associated with gating, are generally unattainable by atomistic equilibrium MD without the use of tailor-made software. The Shaw Group has pioneered the production of millisecond long unbiased simulations by the development of the Supercomputer Anton, optimised for use with MD software.[13] However, this technology is not widely available, leading to the development of alternative approaches to accelerate sampling.

Using a reduced representation is one such approach, utilizing classical MD simulations, to increase the speed and hence timescales obtainable, as well as simulate larger systems with increased complexity. Coarse-grained (CG) molecular

dynamics, as this is known, reduces the number of degrees of freedom in a simulation system by treating a group of atoms as a single entity, significantly curtailing the computational expense of each step. To convert an all-atom structure to a coarse-grained model, hydrogen atoms are not considered, with a number of heavy atoms (typically three or four) grouped into a single interaction site, known as a 'bead'. Interaction potentials are then characterised dependent on the CG model, with required parameters generally developed to reproduce microscopic properties recorded in atomistic simulations and thermodynamic data derived by experimental means. Originally developed to capture the extended time and large-scale behaviour of membranes, a number of CG forcefields have emerged from the research groups of Klein,[14-15] Marrink[16-17] and others.[18] The implementation of these schemes reduces the number of required calculations, as well as increasing the timestep of each iteration (20-40 fs) providing a powerful tool to accelerate molecular simulations. Methods to maintain a level of chemical specificity are also embedded in each scheme; in the Martini forcefield, from Marrink and coworkers, sites are classified by the chemical nature of the region i.e. polar, non-polar, apolar (a mixture of polar and non-polar groups) and charged, for example. Additional techniques are often required to sample phenomena where both atomistic and coarse-grain methodologies are not appropriate, such as those that occur on an extended timescale or involve an energetic barrier.

From MD trajectories of the system in time structural and dynamical quantities as well as kinetic and thermodynamic properties can be calculated using the principles of statistical mechanics. Among the thermodynamic quantities, it is the free energy that provides a direct link between statistical mechanics and thermodynamics, and through which other thermodynamic quantities can be obtained. A long-standing method to calculate the underlying free energy of a system is known as free energy perturbation (FEP). In this method, alchemical transformations are performed to overcome energetic barriers, and the relative free energy differences are calculated by a thermodynamic cycle.[19-20] Several algorithms also exist to accelerate sampling along a pre-defined set of reaction coordinates and estimate the potential of mean force (PMF), such as umbrella sampling, metadynamics, adaptive biasing force or

steered MD. Such reaction coordinates, known as collective variables (CV), are chosen to elucidate a specific conformational transition. A free energy estimate as a function of the collective variables, as well as the equilibrium properties, can be obtained providing a wealth of information about the simulation system at a fraction of the expense of traditional all-atom MD.

Umbrella sampling (US)[21] is perhaps one of the most popular enhanced sampling method in this field, where a bias potential along user-defined CVs provokes conversion between stable thermodynamic states. Independent MD simulations are performed at intermediary steps, known as windows, which can be combined using the weight histogram analysis method (WHAM)[22-23] or umbrella integration.[24] Each window represents equilibrium sampling of energetically distinct locales; accordingly such evaluation estimates the consolidated equilibrium free-energy surface.

Another method in this group is steered molecular dynamics (SMD) simulations.[25] SMD are akin to well-established experimental techniques, such as atomic force microscopy or optical tweezers, where an atom is external force is applied to an atom, or group of atoms, to overcome barriers and sample a specific process.[25] Relative free energies can then be obtained by the Jarzynki equality.[26]

In metadynamics, a superficial bias potential is utilised to advance sampling along suitable CVs, diverting from configurational space previously inhabited. The biasing potential is adjusted by the addition of a Gaussian function, augmenting the energy of the system and departing from local free energy minima, allowing the exploration of alternative thermodynamic states separated by energetic barriers. Once convergence has been achieved, effectively when the entire free energy profile has been flattened, it can be easily reconstructed to provide an unbiased estimate of the landscape as a function of the CVs.

The adaptive biasing force method (ABF)[27] is largely based on thermodynamic integration, whereby the instantaneous force along the reaction coordinate is evaluated directly and counteracted by an external biasing force of equal and opposite magnitude. This effectively provides a smooth energy landscape, and uniform sampling irrespective of energetic barriers allowing accelerated dynamics.

In the following sections, a wide range of literature will be discussed to illustrate how conventional and accelerated MD methods have been used to provide crucial insights into the functioning of the plasma membrane and its constituents on an atomistic level.

Unassisted Diffusion Across Lipid Bilayers

In the first instance, MD simulations have become an established tool to characterise unassisted transport across lipid bilayers, as a model for the biological membrane. The properties of lipid bilayers are generally characterised by a hydrophilic exterior and hydrophobic interior, favourably interacting with aqueous intra- and extracellular compartments (Figure 2A). In reality, of course, the situation is significantly more complex; membranes are highly heterologous systems that are capable of transporting small solutes and impermeable to many others. Even though overall permeability coefficients can be obtained by experimental and computational means, the latter is required to explicitly represent structural and dynamical fluctuations across lipid bilayers and, hence, gain atomistic mechanistic details of transport phenomenon. Although embedded proteins are instrumental in a manifold of transport events as described in later sections, unassisted diffusion is the prevailing manner by which small molecules, including drugs, gain access to the cell. In the following section, we aim to review a selection of recent publications to illustrate the use of computational simulations to explore membrane permeability properties. Model membranes comprised of a single species of phospholipid, such as 1-palmitoyl-2-oleoyl-sn-glycero-3-phosphocholine (POPC), 1,2-dioleoyl-sn-glycero-3-phosphocholine (DOPC) and 1,2-dipalmitoyl-sn-glycero-3-phosphocholine (DPPC) are typically used in this context (Figure 2B).

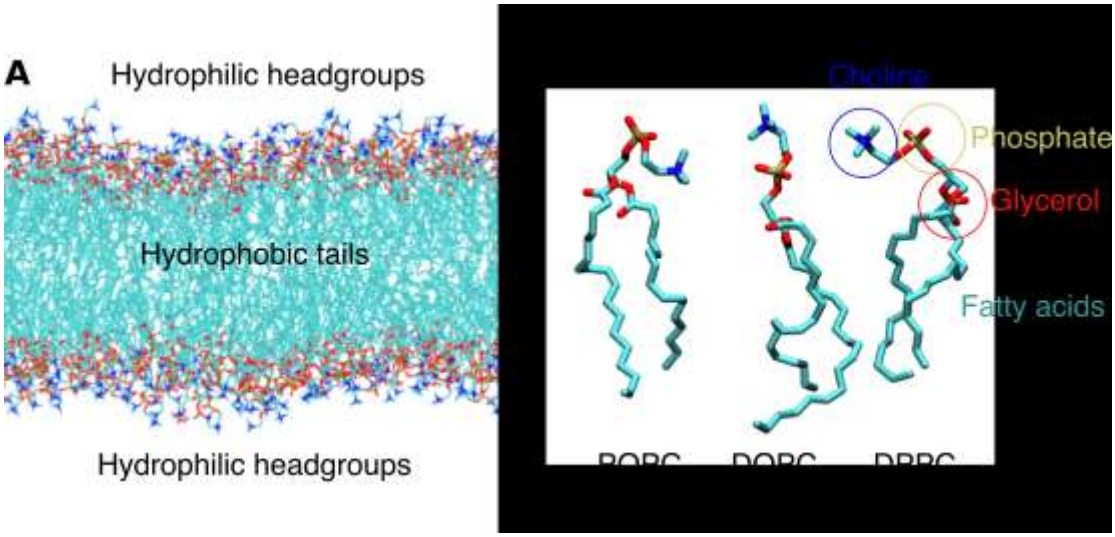

Figure 2. (A) Representation of a single-component lipid bilayer typically used as a model plasma membrane. (B) Structures of common phospholipid molecules used in MD simulations.

Passive diffusion across lipid bilayers is historically characterised by a solubility-diffusion mechanism; the solute diffuses from the extracellular solution and negotiates the membrane prior to accessing the cytoplasm. If partitioning at the membrane-water interfaces is assumed to be at equilibrium, and the membrane is considered as a homogenous oil slab in line with Overton's correlation between membrane permeability and oil/water partitioning coefficient of a solute[28] a simple relationship between the oil/water-partitioning coefficient (K), the diffusion coefficient of the solute in solvent (D) and the membrane thickness can be used to yield the membrane permeability coefficient (P):[29]

$$P = \frac{KD}{h} \qquad \text{Equation 1}$$

The inhomogeneous solubility-diffusion model provides notable improvements by taking into account the heterogeneous behaviour of lipid bilayers, procuring permeability coefficients as a function of membrane depth.[30] Comprehensive sampling of the entire diffusion process is currently unattainable by all-atom MD simulations, due to the computational expense and the stochastic nature of the technique. Therefore, the applicability of this model to MD simulations[31] is dependent on enhanced sampling techniques; the original implementation utilised the z-constraint method[31] whereby the centre of mass of the molecule in question is constrained at defined positions along the z-axis, obtaining free-energies and depth-

dependent diffusion coefficients as a function of the constraining force required at each position. Methods outlined in Computational Methods such as umbrella sampling[21] can also be applied. Such practices remain commonplace today, with alternative techniques to calculate such parameters emerging in recent years.[32-34]

The earliest studies utilising MD simulations to probe passive diffusion primarily focused on small molecules, such as water, oxygen and carbon dioxide.[31] The predictions obtained qualitatively agreed with known transport phenomenon of such molecules: oxygen and carbon dioxide are able to permeate relatively unhindered, where as water diffusion is impeded and therefore, requires aquaporins for fast and efficient transport. This analysis was extended to the most common functional groups. However, the inaccuracy of observed permeability coefficients was notable in comparison to experimental determinations. Fortunately, advancements in computer hardware and empirical forcefields have enabled the characterisation of transport properties to be undertaken at increasing timescales and levels of accuracy.

In a recent study by Riahi and Rowley,[35] the permeability of water and hydrogen sulphide was evaluated using the Drude polarisable model, where experimental diffusion coefficients have been used to optimise parameters for both substances[36,37-38] and the lipid DPPC.[39] Incorporation of induced polarisation effects enabled agreement between calculated and experimental diffusion coefficients at a value of (2.6 ± 0.5) x 10^{-5} cm/s for water,[40] previously calculated as two orders of magnitude greater by additive forcefields.[41] In comparison, a coefficient of 11.9 ± 0.7 was obtained, suggesting hydrogen sulphide permeates approximately 400,000 times faster, and reinforcing experimental suggestions that hydrogen sulphide is at least four orders of magnitude greater than water[35] rendering facilitated transport unnecessary.[42] This is attributed to distinct energetic barriers arising from electrostatic contributions (27 kJ/mol for water vs. 2.6 kJ/mol for hydrogen sulphide); the dominant hydrogen bonding character of water cannot be obtained in the hydrophobic tail region disfavouring the permeation of individual molecules; in contrast, hydrogen sulphide is relatively hydrophobic, thus hydrogen bonding capabilities with water are limited, and occupation of the inner membrane is

encouraged. Therefore, hydrogen sulphide demonstrates permeability on a similar scale to non-polar solutes,[43] undeterred by its innate polarity. This phenomenon likely contributes to the remarkable potency of hydrogen sulphide in biological systems.[44]

The inherent relationship between membrane permeability and biological activity is also important in a drug discovery context. Penetration of cell membranes is imperative to gain access to target sites; the evaluation of permeability coefficients and free-energy profiles of drug molecules evaluation, in a similar manner to small molecules, can be used to assess the likelihood of reaching such sites and hence elicit a functional response. Experimental determination of drug permeabilities requires intensive experimental techniques, thus a plethora of computational studies to characterise the behaviour of clinically relevant molecules in model membranes have emerged to complement experimental work. A chemically diverse range of molecules has been investigated, establishing the partitioning properties of a broad spectrum of drug classes. Orsi and Essex, for example, demonstrated steroid hormones are centralized in the glycerol region, where as, β-blockers tended towards the headgroup region, due to favourable interactions between the central oxygen's and polar moieties in the membrane.[45] Overall, a general consensus has emerged that large drug molecules primarily accumulate at the extended polar/apolar interface to accommodate their amphiphilic nature.[46] Such molecules are found to have a lower energy than in bulk water, with small barriers to overcome, providing an energetically permissible route for drug transit. The calculated ΔG values can sometimes diverge from those determined experimentally, which could be attributed to the use of bilayers containing a single species of lipid and/or consideration of a single drug molecule in the majority of models, even though simultaneous diffusion of a number of molecules may actually occur.[47]

The interrelationship between solute concentration and membrane permeabilities has been examined via MD simulations. Comparison of ABF-generated free energy profiles of the anti-cancer drug, paclitaxel permeation through a pure POPC bilayer and POPC bilayers containing 12 mol % paclitaxel suggested incorporation of paclitaxel endorsed the transportability of the drug by increasing the partitioning

from water to the bilayer (~9 vs~21 kcal/mol) and decreasing the barrier to transfer between leaflets in the bilayer (~7 vs. ~4 kcal/mol).[48] In the paclitaxel-rich bilayers, aggregates are formed from both random and lattice-based starting configurations, which decrease the lipid tail order parameter and promote translocation of water into the membrane, confirming earlier experimental predictions of pore formation in a concentration-dependent manner.[49]

The ability of small membrane bound molecules to cause significant perturbations in membrane structure and accelerate drug permeation has been exploited particularly where transdermal drug delivery is concerned.[50] Molecules such as dimethyl sulfoxide,[51] ethanol,[52] acetone[53] and oleic acid[54] have been proposed as chemical penetration enhancers, to breach the skin barrier by improving permeability of the lipid bilayers of the stratum corneum. The molecular mechanisms by which such molecules act have been investigated in a number of computational studies to date.[55-61]

Dimethyl sulfoxide molecules, for example, were found to freely partition into bilayer and accumulate beneath the lipid headgroups, swelling the distance between adjacent headgroups and dispersing the tails, increasing membrane flexibility and decreasing thickness.[55] Above a certain concentration threshold structural defects generate transient water pores, in a similar manner to paclitaxel, with a further increase expelling individual lipids from the membrane and destroying the bilayer structure.[56] The concentration dependence of dimethyl sulfoxide permeability enhancement experimentally[52] and for pore formation computationally suggests the two phenomena could be related, providing a feasible explanation for the amplified permeabilities of both hydrophobic and hydrophilic compounds through the skin.[52] Comparison of DPPC and DOPC showed that the latter is less susceptible to these effects, demonstrating enhanced stability and diminished dimethyl sulfoxide diffusion.[57]

These examples demonstrate how computational methodologies have provided a mechanistic understanding of experimentally established phenomenon, such as the exclusion of charged and hydrophilic molecules, the partitioning properties of hydrophobic drug molecules and membrane perturbations as a result of molecule

entry. The alternative entry routes to membrane passage, via embedded proteins, will be explored in the following sections.

Passive Transport by Ion Channels

Ion channels facilitate the passive diffusion of ionic species down their electrochemical gradient from the extracellular medium into the cell cytoplasm. Permeation is controlled by the onset of various external stimuli, such as transmembrane voltage, heat, ligand binding, and mechanical stretch, and is responsible for regulating electrical signals across the cellular membrane.

The voltage-gated ion channel (VGIC) family that specifically conduct Na^+ (Na_V channels) and K^+ ions (K_V) channels, for example, are responsible for the generation of action potentials in excitable cells in various tissues in the heart, brain and nervous system, and thus play a crucial physiological role. VGIC's are a common target for antiarrhythmic agents, local anaesthetics, anticonvulsants and pain therapeutics.[62-63] Understanding how such proteins assemble and function is therefore of great pharmacological importance.

Elucidation of the crystal structure of the KcsA channel from *Streptomyces lividans* in 1998, provided the first atomistic description of the pore structure of an ion channel, a tetrameric arrangement with each monomer containing two transmembrane α-helices and an intermittent pore loop (Figure 3).[64] The latter was found to contain a pore helix and the signature selectivity sequence and thus has become known as the selectivity filter.[65-66] Between the selectivity filter and the cytoplasm, a water-filled cavity is present to provide an ideal environment for ion transfer.[67] MD simulations, using KcsA, have extensively analysed the mechanism by which K^+ channels selectively and efficiently conduct K^+ ions.[68-72] The abundance of K^+ channel structures now available has enabled various aspects of K^+ channel function, such as voltage-sensing, cytoplasmic gating and drug blockage to be examined by computational analyses.[73-75] Several comprehensive reviews are available on this subject.[76-77] Similarly, since the publication of the first crystal structure of the Na_VAb from *Arcobacter butzleri*,[78] and subsequent structures from bacterial sources,[79-82] significant efforts have been focused towards elucidating analogous functional properties in NaV channels. The pore structure of NaVAb showed similar

characteristics to K_+ channels, displaying a voltage-domain attached via a linker domain, as shown in Figure 3. In this section, recent insights gained from the Na_VAb channel will be used to illustrate the application of computational methodologies to complex questions regarding ion channels.

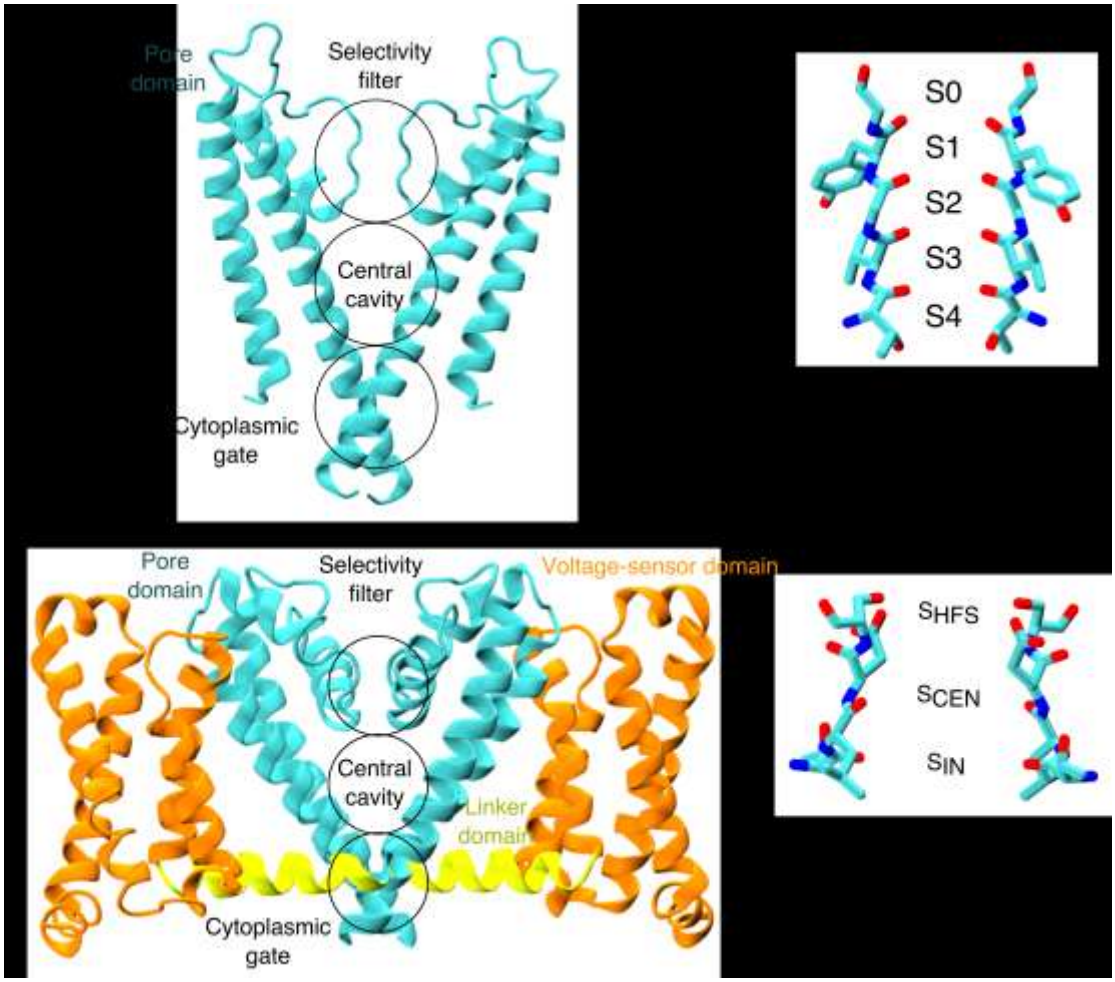

Figure 3. (A) Structure of KcsA potassium channel. (B) Proposed ion binding sites in the KcsA K^+-channel selectivity filter. (C) Structure of voltage-gated sodium channel Na_VAb. (D) Proposed ion binding sites in Na_VAb Na^+-channel selectivity filter. Only two domains are shown for clarity throughout.

The resolved selectivity filter structure identified three possible ion-binding sites which were apparently capable of coordinating partially hydrated ions; at the extracellular entrance, the S_{HFS} site formed of a ring of anionic glutamate residues Glu177, was proposed to attract extracellular cations; deeper sites proposed (S_{IN} and S_{CEN}) were composed of carbonyl backbones Leu76 and Thr175 respectively (Figure 3D). The observed ion dynamics in early MD simulations was consistent with

predictions from structural data.[83] The binding sites were also confirmed as energy minima in single and multi-ion PMF conduction profiles [84-85] and later MD simulations on a microsecond timescale. The conformation of the residues forming the binding sites was largely unchanged irrespective of the presence of ions,[86] in contrast with K^+ channels whose sites depend on the presence of K^+ ions for stability.[87-89]

The precise sequence of events inducing Na^+ conduction was examined via umbrella sampling calculations, sampling conduction along the permeation axis. As expected, a deep energy well between –5 kcal/mol [90] and -8 kcal/mol[85] was observed at S^{HFS}. Entrance to further sites, however, was subject to a barrier of 4 kcal/mol [90 85], suggesting movement of isolated ions was not the primary mechanism of conduction, as proposed from flux measurements.[91] Accompanying multi-ion profiles displayed an reduced energy barrier below 3 kcal/mol for penetration of the selectivity filter, advocating translocation of Na^+ ions likely occurs via sequential movement through doubly occupied extracellular/S_{HFS}, S_{HFS}/S_{HFS}, S_{HFS}/S_{CEN}, S_{HFS}/S_{IN}, S_{HFS}/intracellular conformations, in a so-called loosely coupled 'knock-on' mechanism. Additional efforts to characterise the minimum energy pathway utilizing metadynamics, taking into account binding as a function of the radial distribution around the pore axis, identifying an additional 'drive-by' mechanism of conduction.[92] Extensive MD simulations of ~22 μs in the absence of a transmembrane voltage, provided direct observations of knock-on/off transitions, multi-ion configurations constituted over 90% of the simulation trajectory.[93] Interestingly, more than 20% were triply occupied states of the selectivity filter, which have also been observed in bias-exchange metadynamics simulations.[94]

The presence of such states has been associated with conformational states of the selectivity filter, divergent from the crystal structure. Multi-microsecond simulations revealed Glu177 could occupy an additional conformational state directed towards the selectivity filter, as opposed to the extracellular medium, which is thought to catalyse Na^+ permeation.[93] Boiteux et al disclosed PMF profiles with a double energy well at this site, resulting in reduced energy barriers, supporting this proposal.[95] An increased occupancy of the selectivity filter is observed in this case, providing further

evidence of a conduction mechanism involving three ions. Studies have since proposed distinct multi-ion conduction mechanisms may be in operation during inward and outward conduction.[96]

The protonation state of Glu177 has also been under intense scrutiny throughout MD simulations. Multiple studies utilizing both equilibrium[95] and free-energy MD.[84 97] methodologies conclude conduction is favoured in the wholly deprotonated state, and is unfeasible when multiple residues are protonated.

The mechanism by which Na^+ channels exclude other monovalent and divalent ions has been explored by comparison of single and multi-ion PMF profiles.[84-85] These profiles demonstrated that even though K^+ ions were capable of penetrating the channel with a favourable network of coordinating ligands, a heightened barrier was identified in the plane of the Glu177 side-chains.[84] This observation was rationalised using geometric arguments, as K^+ is unable to permeate this region unperturbed in an optimum geometry, and supported by a systematic comparison between selectivity and pore radius in the same study. The overall free-energy difference for K^+ relative to Na^+ was calculated as 3 kcal/mol in line with experimental permeability ratios. PMF profiles of Ca^{2+} conduction displayed distinct energy landscapes from both Na^+ and K^+, suggesting further mechanisms of selectivity in the Na_V filter. Corry et al proposed the desolvation energies of Ca^{2+} likely results in hindered permeation;[90] in addition, Ke et al advocated that transfer from S_{CEN} to the central pore was energetically unfavourable, thus sustained inhabitancy of this site blocks inward conduction of Ca^{2+}.[98]

As well as exploring mechanistic aspects of NaV channel conduction and selectivity, aspects of channel modulation have also been explored computationally. NaV channels represent a putative target for local and general anaesthetics, yet the functional binding sites of such molecules, and the pathway by which they can access them are not widely understood. A multitude of experimental studies have proposed the existence of a 'hydrophobic pathway' enabling the entrance of hydrophobic molecules, when entrance is obstructed from both extracellular and intracellular vestibules.[99] The Na_VAb structure revealed the presence of hydrophobic side-portals, termed fenestrations, thought to represent such a route. Thus, the

dynamics of these sites and their accessibility to drug molecules have been the focus of several studies in recent years.

Using a structural model of NaChBac, Raju et al identified three binding sites of the general anaesthetic isoflurane, in the extracellular, linker and pore domains using flooding simulations, with subsequent FEP calculations to estimate the free energy of binding of each site.[100] Entry/exit routes were observed on the fly, including traversal of the fenestrations to the central pore site, confirming the feasibility of the portals as access pathways. The evolution of the size and dynamics of the fenestrations and hence, the size restrictions imposed on incoming drug molecules were subsequently explored by Kaczmarski and Corry.[101] A range of bacterial NaV channels displayed an average bottleneck radii between ~1.6 and 2.2 Å, reaching a maximum bottleneck radii between ~2.6 and 2.8 Å. Thus, in the maximally extended state, the portals are capable of accommodating phenyl rings, a key constituent of most sodium-channel blocking drugs.[102] Entrance of larger drugs would, therefore, require considerable perturbations of the fenestration or drug conformation. In NaVAb, F203 acted as the central gate to fenestration size, illustrating that fluctuations in bottleneck radii are primarily determined by rapid side-chain rotations. The entrance of lipid molecules was also found to modulate fenestration size and dynamics. Further studies investigated access of the local anaesthetic benzocaine and the anti-epileptic drug phenytoin to the central pore; in agreement with the predicted physical constrictions, free energy maps constructed from umbrella sampling simulations,[103] and extensive unbiased MD simulations indicated a larger barrier for the entrance for the larger phenytoin, although both exhibited a minimum energy pathway through the lateral fenestrations.[104] The possible existence of lateral fenestrations in K^+ channels has subsequently been investigated using MD simulations, identifying tuneable openings in the two-pore domain K^+ channel family.[105]

In conclusion, MD simulations have revealed key principles of ion conduction in bacterial Na_V channels. It is now understood that permeation at high-throughput requires two ions at a minimum, which are loosely coupled with each other and water molecules in the selectivity filter, in stark contrast to K^+ channels.

Furthermore, lateral fenestrations have been confirmed as viable entry routes for small hydrophobic molecules to reach high-affinity binding sites in the central pore. The molecular determinants of conduction and selectivity of Ca^{2+} channels are yet to be distinguished, and will likely be the subject of computational studies when high-resolution structural information is available.

Facilitated Diffusion by Transporters

Membrane transporters are a highly specialised class of membrane proteins, which couple substrate translocation to a variety of cellular energy sources. A wide range of chemical species are admitted passage via transporters, often against the electrochemical gradient of the plasma membrane. This process is thought to occur by means of an *alternating access* mechanism, whereby the transporter interior is sequentially exposed to the intracellular and extracellular frontiers of the membrane. Primary transporters utilise energy input directly from chemical reactions, whilst secondary transporters derive are driven by an electrochemical gradient. MD simulations have provided considerable insights into the interrelationship between transporters and chemical driving forces, and how this is coupled to the large-scale conformational changes underlying the alternating access model. In this section, we have limited our discussion to the Leucine transporter (LeuT), which has become a prototype for structural and dynamical analyses of neurotransmitter sodium symporter (NSS) family, to illustrate the progression of our understanding in this field.

NSS's are responsible for the selective re-uptake of substrates to terminate neurotransmission at synapses.[106] These transporters function in a Na^+ dependent manner, coupling the passive diffusion of Na^+ down the electrochemical gradient, to the active transport of substrate molecules, including monoamine neurotransmitters (serotonin, dopamine, norepinephrine), amino acids and osmolytes (betaine, taorine, creatine). Eukaryotic NSS are the pharmacologically as targets for important drugs, such as anti-depressants,[107] as well as psychoactive substances, such as cocaine.[108] Determination of the structure of the bacterial amino acid transporter LeuT elucidated the basic transmembrane architecture of NSS's,[109] denoted the 'LeuT fold', comprised of two five-helical bundles in an anti-parallel arrangement (Figure 4A).[110] A wealth of atomic resolution structural information of LeuT from *Aquifex aeolicus* has since emerged,[111-114] revealing various novel aspects of NSS assembly. The available structural information advocates a mechanism of alternating access in which Na^+ ions and the substrate bind to an outward-facing open (OF_O) state, and released by a series of concerted transitions between outward-facing

closed (OF_C), inward-facing closed (IF_C) and inward-facing open (IC-O) states, where the transporter can loop back to the initial conformation. The availability of LeuT structures has allowed in-depth investigation of its behaviour by MD simulations, as a paradigm for the NSS transporter function.

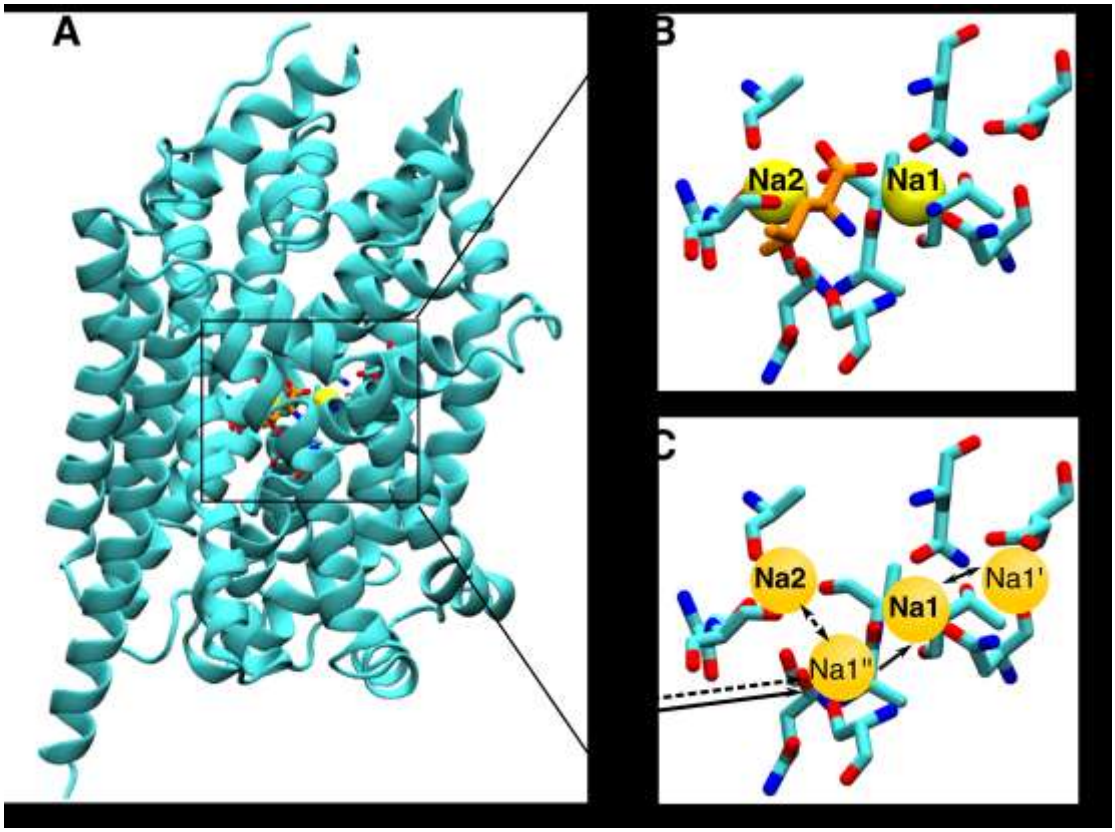

Figure 4. (A) Crystal structure of LeuT receptor in OF_C conformation with two Na^+ ions and leucine bound. (B) Close-up of substrate and ion binding sites. (C) Proposed sequence of ion binding; straight and dashed lines represent the movement of the first and second ions respectively. Throughout, protein residues are shown in licorice representation, with blue, red, cyan and orange parts representing nitrogen, oxygen, carbon in LeuT and carbon in leucine. Sodium ions are shown as yellow spheres.

Crystallographic information of LeuT has elucidated the presence of two Na^+ binding sites (Na1, Na2), in close proximity to the substrate-binding site (S1) in the membrane core (Figure 4B).[110] Na1 explicitly coordinates the substrate, alongside residues Ala22, Asn27, Thr254 and Asn286 in an octahedral arrangement. In contrast, Na2 is entirely composed LeuT residues (Gly20, Val23, Ala351, Thr354 and Ser355), coordinating ions in a trigonal bipyramidal manner. In the initial computational studies, the dynamics of such sites was investigated.

In the first MD study, Celik et al performed a series of unbiased MD simulations on the initial crystal structure of an OF_C, which contained the bound substrate and two Na^+ ions, to explore dynamics of this LeuT complex.[115] The most notable interactions in the observed substrate binding process of the zwitterionic leucine involved a salt bridge in the extracellular vestibule (Arg30 and Asp404) and an ion occupying Na1 on occupation of the canonical binding site. FEP/MD simulations were undertaken by Noskov and Roux to discern the mechanism by which other cations are excluded from Na^+ binding sites, and hence the specificity of LeuT to Na^+ ions.[116] Interestingly, distinct mechanisms of selectivity were observed; in Na1, coordination to a negatively charged residue results in preferred binding of Na^+, where as geometric constraints were proposed to operate in Na2. The influence of ion occupation on substrate binding was also assessed using FEP simulations, revealing optimum substrate coupling to Na^+ when both sites are occupied, and enhanced structural stability of the substrate and Na^+ site selectivity when Na2 is inhabited.[117]

Celik also undertook a series of steered MD experiments to probe the formation of IF_C complex. Entrance to the site required an open state of the aromatic lid (Phe353), which closed upon stable binding, thus illustrating as a key transition between OF_O and OF_C states.[115] Later unbiased simulations of the OF_C state, with the substrate removed, displayed spontaneous opening to a conformation poised for substrate binding, similar to the OF_O crystal structure, demonstrating Na^+ binding in isolation to biases the transporter towards this state and further elucidating the conformational changes involved in this transition.[118] The authors noted that the affinity for Na1 is inversely proportional with the progression of the transition of the IF_O state, thus it is likely occupation of Na2 contributes to the stability of this conformation. This has recently been confirmed by mutagenesis of the Na2 site (Thr354 and Ser355), which was found to stabilize the IF_O state by direct interactions with helices 1 and 8.[119]

Computational analyses have also been able to predict additional Na^+ sites, not identified during crystallographic data, in order to delineate the precise series of events constituting Na^+ and substrate entrance (Figure 4C). Zhao et al identified an additional binding site in close proximity to Na1 located on Glu290, referred to as

Na1' from this point forward.[118] The evolution of the protonation state of Glu290 is known to be an integral part of the transport cycle, corroborating this prediction.[120] Using extensive all-atom MD simulations (~20 μs), Zomot et al identified an additional binding site, namely Na1'', constituted of Ser256 and Ser355 side-chains and the backbone carbonyl of Asn21, and have provided an exhaustive account of Na^+ translocation events, and associated conformational changes.[121] Site Na1'' appears constitutes the first point of contact for Na^+ ions, attracting anions from the extracellular medium throughout; within hundreds of nanoseconds, this ion shifts to Na1 where it maintains residence, or transiently occupies Na1'. The Na1'' site may remain vacant whilst Na1 is occupied, or hold a further incoming ion, which can subsequently enter Na2. Simultaneous population of both sites is consistently correlated with expansion of the extracellular entrance, permitting access of the substrate to S1. Following binding, the entrance is concealed by local rearrangements, notably the side-chain isomerization of Phe253. Subsequently, the surrounding helices undergo global rearrangements to evolve conformations capable of releasing the bound species.

In the OF_O state, Zhao and Noskov observed the formation of water wires from the cytoplasm to the to the S1 and Na2 sites in the IF_O state, may facilitate ion release and prompt inter-helical arrangement and flooding of the intracellular opening.[122] Using free energy calculations, Thr345 was shown to occupy single rotameric state when Na2 is occupied, as opposed to two degenerate states when it is vacant, and thus may act as a switch to vacate Na2 and advance the transport cycle.

Significant efforts were directed towards prediction of further intermediates in the transport cycle, such as the IF_O structure. [123-125] Tajkhorshid et al produced an IF_O model by homology modelling of the inward-facing state,[126] based on the structures of outward-facing LeuT[110] and inward facing vSGLT [127]. Simulations of this state consistently displayed intracellular release of Na2. Quick et al proposed a similar structure, in addition to other unknown states, by varying the presence of leucine in the binding site and Na^+ ions in known crystal structures and performing accelerated MD simulations in combination with principal component analysis.[123] All inward-facing conformations were found to contain a vacant Na2 site. The eventual

crystallization of a LeuT inward-facing state[111] further corroborated earlier predictions that Na2 initiates intracellular release; Na^+ ions were weakly coupled with the Na2 site, persistently exiting to the intracellular medium and initiating release of the bound substrate and ion in Na1 in the same direction.[128] The protonated/neutral state of Glu290 (Na1' site) in the inward-open state is proposed to enhance dissociation of ions to the intracellular solution.[129] These observations provide a mechanistic understanding of how negative charges in close proximity to the characteristic Na^+ binding sites, such as Glu290 in the LeuT transporter or chloride ions in eukaryotic NSS, may regulate ion binding and release.[120]

The overall mechanism of release has been a source of controversy throughout the literature. Early SMD simulations by Shi et al revealed a second substrate-binding site (S2), leading to proposals of an allosteric mechanism of transport whereby occupation of the secondary binding site, triggers release of the inhabitants of S1 and Na1.[130] Furthermore, the observed overlap of the S2 site with the binding site of tricyclic antidepressants has lead to suggestions that the S2 site could exert an activator or inhibitory effect dependent on the manner of binding.[112-113]

Championed by Javitch and Weinstein,[130-132] the presence of the S2 binding site has been widely disputed throughout the literature, with Gauaux and coworkers, for example, endorsing the functional significance of the S1 site only.[110, 133-136] Differing reports have also emerged in computational studies. Extensive unbiased simulations by Zomot et al, do not observe alanine binding, and only partial leucine binding in the S2 site.[121] On the other hand, using a complex protocol combining of accelerated, targeted and conventional MD, Cheng et al have identified an increase in the substrate-binding affinity of the S2 site whilst progressing towards an inward-facing state and subsequent displacements in the putative S1 site.[137] Furthermore, unbiased simulations with Ala and Leu and inhibitors known inhibitors bound at the S2 site revealed key structural alterations in the extracellular portion of TM6 which may be propagated throughout the transporter and influence its functional state.[138] FEP/MD simulations yielded favourable absolute binding free energies for tricyclic antidepressants in the range of -12 to -14 kcal/mol.[139] These energies were dissimilar

on removal of the substrate, supporting a thermodynamic coupling mechanism between the two sites.[112]

The final question remaining of LeuT transport involves the inward-to-outward transition to restart the translocation mechanism. The recent crystallization of WT LeuT in a Na^+ and substrate-free state by Malinauskaite et al provided the first insights into the structure of an intermediate involved in this transformation.[114] MD simulations confirmed both Na^+ sites are inaccessible to extracellular ions in the structure, with a distinct Na1 conformation observed stable throughout. Highly conserved residue, Leu25, is found to consistently occupy the S1 site, and occlude Glu290 from the extracellular environment, reportedly acting as gatekeeper for Na^+ binding and playing an intimate role in H^+-counter-transport during the return transition. The authors propose release of the counter-ion stimulates reorientation of Leu25, allowing entry to the sites and initiation of the forward transport cycle.

Remarkably, using the available crystal structures of LeuT, MD simulations have provided a full atomistic description of the entire transport cycle. Key questions concerning the locality and behaviour of Na^+ binding sites, the interrelationship between such sites and substrate binding at different stages of the transport cycle, as well as a possible allosteric mechanism involving a second substrate-binding site have been addressed.

In a wider context, these studies have examined the key principles of membrane active transport: molecular determinants of substrate binding, coupling to external energy sources and conformational changes constituting the alternative access mechanism. These fundamental principles of active transport have been examined in a number of transporter families, and it is likely that a detailed description of active transport in these assemblies will emerge in the future.

Signaling via Receptors

Cell surface receptors are intrinsic membrane proteins forming the primary communication mechanism between the cell exterior and interior. The functionality of receptors is dependent on the transformation of the protein transmembrane between conformational states, in response to the binding of extracellular

molecules. Ligand-gated ion channels are a family of membrane receptors that allow ion influx/efflux in response to bound neurotransmitters. G-protein coupled receptors (GPCR's) constitute a significant class of membrane receptors, which couple to heterotrimeric G-proteins on activation to initiate intracellular signalling cascades. GPCR's are susceptible to hormones, neurotransmitters, and sensory stimuli, thus they are critical for basic physiological function of eukaryotic organisms.[140] As a consequence, GPCR's have been implicated in neurological disorders, cardiac failure, cancer and diabetes, and are the target of a significant proportion of pharmaceuticals available on the market today.[141-142]

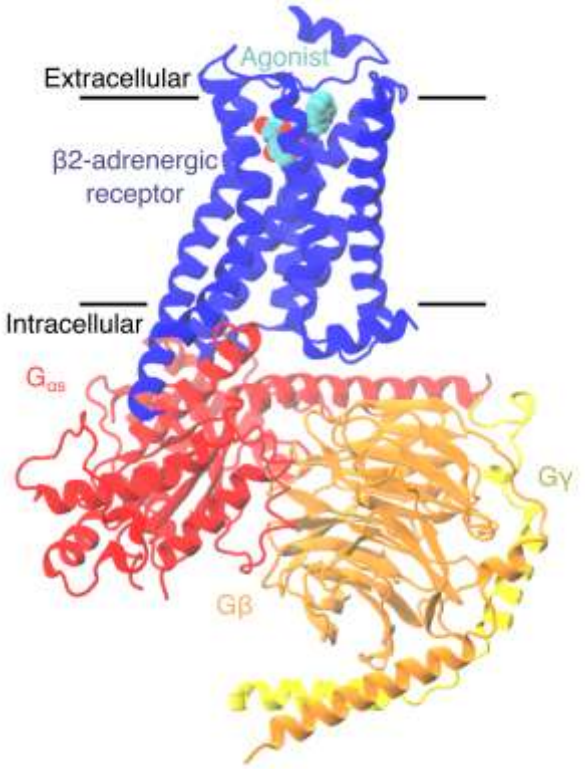

Figure 5. Crystal structure of β2-adrenergic receptor (PDB ID 3SN6) in fully activated state with bound agonist and heterotrimeric G-protein. The position of the plasma membrane is indicated by a solid black line.

As GPCR activation is a profoundly dynamic process reliant on large-scale conformational changes, elucidation of high-resolution three-dimensional structures has proven difficult.[143] The ground breaking crystal structure of light sensitive pigment, rhodopsin, revealed the conserved transmembrane arrangement of seven α-helices of class A GPCR's and provided high-resolution data appropriate for MD

simulations. In recent years, computational analyses of GPCR's has been significantly aided by the increase in X-ray crystallographic information and state-of-art homology modelling tools, exploring numerous facets of GPCR behaviour, such as ligand binding, G-protein coupling, lipid modulation the highly concerted conformational changes associated with activation/inactivation processes. The β2-adrenergic receptor has been the focus of seminal studies exploring the latter, due to the availability of structural information in multiple functional states, including a fully activated state in complex with extracellular agonist and intracellular G-protein complex (Figure 5). Thus, it will be used as an archetypal example of how computational methodologies have advanced our understanding of the relationship between GPCR structure and function.

Multiple studies have advocated that an ensemble of conformational states exist for individual GPCR functional states.[144-145] The initial β2AR structures, in complex with inverse agonist carazolol and timolol,[146-149] allowed theoreticians to characterise the ensemble of conformational states representing the inactive state of the receptor.[150] Unexpectedly, a salt bridge between the intracellular ends of helices III and VI, dubbed the 'ionic lock', was broken in the inactive state structures, in defiance of biochemical evidence arguing this event represents a crucial activation step.[151] Microsecond simulations of these structures were able to demonstrate that inactive β2AR actually exists in conformational equilibrium between states with a broken and intact ionic lock.[150] These observations suggest the receptor is likely biased towards the broken state upon receptor activation, reconciling with the previous experimental work mentioned.[151]

The elucidation of the agonist bound β2A receptor lead to further investigation of GPCR conformational states and the transitions between them. Rosenbaum et al explored the dynamics of this complex on an extended timescale using the Anton Supercomputer.[152] This seminal study demonstrated the feasibility of simulations up to 30 μs in length for the study of integral proteins, and provided unprecedented insights into the behaviour of this complex. After approximately 11 μs, the active state receptor spontaneously transitioned to the inactive structure that remained stable for the duration of the simulations, advocating that binding to an intracellular

partner was absolutely required for stabilization of a fully activated conformation. Later experimental and computational works supported this hypothesis.[153]

Dror et al proposed an atomically detailed activation mechanism based on the transition between functionally active and inactive states, via a number of previously unreported intermediates, observed reproducibly in over 30 independent simulations.[154] Three functionally important regions were identified, the intracellular G-protein-binding site, the extracellular ligand-binding site and the junction in between, the so-called 'connector' region. The regions are loosely coupled, although the connector region is largely responsible for communicating small-scale ligand related movements and large-scale helical movements surrounding the intracellular binding pocket. Interestingly, the simulations suggest the activation process originates from the latter; outward movements of helix VI initiate conversion to an intermediate state, which incorporates an expanded G-protein site, and an equilibrium between active and inactive states in the ligand binding site and connector region. Subsequent agonist binding biases this equilibrium towards active conformations. Finally, an intracellular binding partner may interact and trigger the final stage of the activation process. Detailed understanding of specific receptor conformations, as described here, may contribute to the design of drugs targeting specific functional states of GPCR's. Knowledge of the interrelationship between cellular entities, such as G-proteins and arrestins, and the multitude of conformational states of the β2AR will refine this scheme further.

A key question that has not been addressed throughout these mechanistic studies is the assembly of GPCR dimers and higher-order oligomers, and their functional role of in the intracellular signalling pathway. Hydrophobic mismatch, where the length of the membrane spanning segments conflicts with the length of the hydrophobic core of the membrane, has been proposed to stimulate GPCR dimerization, and has consequently been explored using MD simulations.[155] Using a novel multi-scale approach known as Continuum-Molecular Dynamics, Mondal et al quantified energetic penalties emerging from this phenomenon in individual transmembrane helices of GPCR's, enabling the prediction of energetically favourable contact interfaces by comparison such energetic costs in monomeric and oligomeric

states.[156] In the β2A receptor, the hydrophobic mismatch was considerably reduced in the transmembrane helices I, IV and V consistent with the typical interfacial regions elucidated from unbiased CGMD (helices I-I, V-V and IV-V),157 with similar results obtained using a bilayer containing 10% cholesterol. Duplicate analysis of the β1A displayed distinct oligomerisation patterns, with a single predicted contact interface localized on helix I. Overall, these results were akin to experimental evidence showing the β1A preferentially forms dimers,[158] where as the β2A receptor can form more extensive dimers as well as higher-order oligomers.[159]

Prassanna et al performed extensive CGMD of the β2A receptor in bilayers containing increasing concentrations of cholesterol to examine the effect of cholesterol on the dimerization process.[160] In 0% cholesterol, the receptors form a homo-interface involving helices IV and V; in 50% cholesterol, a homo-interface between helices II and I is formed; whilst in the concentrations between (9 and 30%) a hetero-interface is observed comprising a combination of the two. Increased cholesterol occupancy at helix V is observed throughout, advocating specific cholesterol interaction bias the oligomer towards distinct oligomeric states.

It is well established throughout the literature that functionality of integral membrane proteins is dependent on the composition of the plasma membrane, thus it is possible the influence of membrane organization extends further than GPCR dimerisation. Many GPCR's have demonstrated a functional dependence on membrane cholesterol in particular, which is considered to act either by direct interactions or indirect effects involving the biophysical properties of the membrane.

Unbiased MD simulations, either CG or atomistic, of GPCR's embedded in lipid bilayers enriched with cholesterol molecules have become a popular tool to identify cholesterol binding sites.[161-164] Utilising this protocol, Cang et al revealed the presence of three extracellular and four intracellular high occupancy sites. The accuracy of such predictions was supported by the likeness between three sites and those observed in crystal structures of GPCR's with bound cholesterol molecules. Of note, two cholesterol molecules occupy the surface of helix I and VIII, consistent with that observed in the dimeric structure of the β2AR (PDB 2RH1), contrasting with claims that the observed organization was an artefact caused by crystal packing.[147]

Furthermore, a cleft between the extracellular ends of helices I, II and VII, accommodated a cholesterol molecule in a stable manner for the duration of the trajectories. The authors suggest habitation of this site, and the resulting stabilisation of residue Trp313, may facilitate ligand-receptor binding.

Prasanna et al identified a specific POPC binding site between helices I and VII, in a similar position in the extracellular leaflet.[165] This site had been previously suggested to accommodate lipids from X-ray crystallographic information of the α2-adenosine receptor. Neale et al explored the relational between specific phospholipid interactions and receptor activation state.[161] Using MD simulations with a cumulative time of 0.25ms, the authors observed individual phospholipid molecules entering the receptor by an opening in the cytoplasmic leaflet between helices VI and VII and forming a salt-bridge that directly impedes ionic lock formation, thus stabilizing the active state. This phenomenon was enhanced by the presence of anionic lipids, elucidating a possible mechanism by which such lipids perpetuate receptor activation.

In conclusion, MD has provided crucial insights into how GPCR's convert between functional states to convey signals, as a result of highly synchronized structural transitions emanating from atomic fluctuations. The driving forces of receptor dimerisation have been studied, and the functional significance of higher order oligomers considered. The close association between membrane lipids and receptor state has been explored, with the identification of multiple functional binding sites of both cholesterol and phospholipid molecules.

Conclusions

Molecular dynamics simulations have become an essential tool to study the dynamics of biological systems in atomic resolution, and elucidate the molecular mechanisms of numerous phenomena that cannot be gained by experimental means. A detailed understanding of how many small molecules interact with lipid bilayers, and consequential diffusion or exclusion processes has been gained, which can be applied in a medicinal chemistry context to assess the likelihood of drug molecules reaching intracellular targets. Furthermore, computational methodologies in combination with high-resolution structural information of integral membrane

proteins have provided crucial insights into how such assemblies function as highly efficient transport machinery. For ion channels, multiple conduction mechanisms for selective transport through K^+ and Na^+ channels have emerged, as well as characterisation of a novel pore access pathway through lateral fenestrations in the latter. In the case of GPCR's, conformational ensembles of active and inactive functional states have been described, and the inter-conversion transitions delineated, providing a general mechanism of GPCR activation. The influence of the membrane environment on GPCR dynamics by direct and indirect effects has been explored intensively. Finally, significant advances have been made in understanding the alternating access mechanism underlying transporter function, and how such changes are driven by cellular energy sources. Overall, such insights have considerable contributed to our understanding of membrane transport, and will significantly advance the ration design of drugs in the future. The increasing availability of high-resolution structural information, growth in computer capabilities and development of state-of-the art MD algorithms and accompanying force fields will markedly amplify the use of computational simulations for the study of intrinsic membrane proteins in the coming years.

Acknowledgements

V.O. acknowledges a BBSRC-CASE studentship, in association with Pfizer Neusentis. C.D. acknowledges use of ARCHER, the UK National Supercomputing Service, the National Service for Computational Chemistry Software (NSCCS), the 'Red Española de Supercomputación' (RES), and the Hartree Center. Research in the Domene group is supported by the Engineer and Physical Sciences Research Council (EPSRC) and the Biotechnology and Biological Sciences Research Council (BBSRC).

References

1. Luckey, M., *Membrane Structural Biology: With Biochemical and Biophysical Foundations*. Cambridge University Press: 2014.

2. Brooks, B. R.; Bruccoleri, R. E.; Olafson, B. D.; States, D. J.; Swaminathan, S.; Karplus, M., CHARMM: A program for macromolecular energy, minimization, and dynamics calculations. *Journal of computational chemistry* **1983,** *4* (2), 187-217.

3. Cornell, W. D.; Cieplak, P.; Bayly, C. I.; Gould, I. R.; Merz, K. M.; Ferguson, D. M.; Spellmeyer, D. C.; Fox, T.; Caldwell, J. W.; Kollman, P. A., A Second Generation Force Field for the Simulation of Proteins, Nucleic Acids, and Organic Molecules. *Journal of the American Chemical Society* **1995,** *117* (19), 5179-5197.

4. Jorgensen, W. L.; Tirado-Rives, J., The OPLS [optimized potentials for liquid simulations] potential functions for proteins, energy minimizations for crystals of cyclic peptides and crambin. *Journal of the American Chemical Society* **1988,** *110* (6), 1657-1666.

5. Vorobyov, I. V.; Anisimov, V. M.; MacKerell, A. D., Polarizable Empirical Force Field for Alkanes Based on the Classical Drude Oscillator Model. *The Journal of Physical Chemistry B* **2005,** *109* (40), 18988-18999.

6. Patel, S.; Brooks, C. L., CHARMM fluctuating charge force field for proteins: I parameterization and application to bulk organic liquid simulations. *Journal of computational chemistry* **2004,** *25* (1), 1-16.

7. Patel, S.; Mackerell, A. D., Jr.; Brooks, C. L., 3rd, CHARMM fluctuating charge force field for proteins: II protein/solvent properties from molecular dynamics simulations using a nonadditive electrostatic model. *Journal of computational chemistry* **2004,** *25* (12), 1504-14.

8. Shi, Y.; Xia, Z.; Zhang, J.; Best, R.; Wu, C.; Ponder, J. W.; Ren, P., Polarizable Atomic Multipole-Based AMOEBA Force Field for Proteins. *Journal of Chemical Theory and Computation* **2013,** *9* (9), 4046-4063.

9. Lamoureux, G.; MacKerell, A. D.; Roux, B. t., A simple polarizable model of water based on classical Drude oscillators. *The Journal of Chemical Physics* **2003,** *119* (10), 5185-5197.

10. Lemkul, J. A.; Huang, J.; Roux, B.; MacKerell, A. D., An Empirical Polarizable Force Field Based on the Classical Drude Oscillator Model: Development History and Recent Applications. *Chemical Reviews* **2016**.

11. Miyamoto, S.; Kollman, P. A., SETTLE: an analytical version of the SHAKE and RATTLE algorithm for rigid water models. *J. Comput. Chem.* **1992,** *13* (8), 952-962.

12. Perilla, J. R.; Goh, B. C.; Cassidy, C. K.; Liu, B.; Bernardi, R. C.; Rudack, T.; Yu, H.; Wu, Z.; Schulten, K., Molecular dynamics simulations of large macromolecular complexes. *Current Opinion in Structural Biology* **2015,** *31*, 64-74.

13. Shaw, D. E.; Maragakis, P.; Lindorff-Larsen, K.; Piana, S.; Dror, R. O.; Eastwood, M. P.; Bank, J. A.; Jumper, J. M.; Salmon, J. K.; Shan, Y.; Wriggers, W., Atomic-Level Characterization of the Structural Dynamics of Proteins. *Science* **2010,** *330* (6002), 341-346.

14. Shelley, J. C.; Shelley, M. Y.; Reeder, R. C.; Bandyopadhyay, S.; Klein, M. L., A Coarse Grain Model for Phospholipid Simulations. *The Journal of Physical Chemistry B* **2001,** *105* (19), 4464-4470.

15. Shelley, J. C.; Shelley, M. Y.; Reeder, R. C.; Bandyopadhyay, S.; Moore, P. B.; Klein, M. L., Simulations of Phospholipids Using a Coarse Grain Model. *The Journal of Physical Chemistry B* **2001,** *105* (40), 9785-9792.

16. Marrink, S. J.; de Vries, A. H.; Mark, A. E., Coarse Grained Model for Semiquantitative Lipid Simulations. *The Journal of Physical Chemistry B* **2004,** *108* (2), 750-760.

17. Lopez, C. A.; Sovova, Z.; van Eerden, F. J.; de Vries, A. H.; Marrink, S. J., Martini Force Field Parameters for Glycolipids. *J Chem Theory Comput* **2013,** *9* (3), 1694-708.

18. Saunders, M. G.; Voth, G. A., Coarse-graining methods for computational biology. *Annual review of biophysics* **2013,** *42*, 73-93.

19. Zwanzig, R. W., High-Temperature Equation of State by a Perturbation Method. I. Nonpolar Gases. *J. Chem. Phys.* **1954,** *22*.

20. Beveridge, D. L.; DiCapua, F. M., Free Energy Via Molecular Simulation: Applications to Chemical and Biomolecular Systems. *Annual Review of Biophysics and Biophysical Chemistry* **1989,** *18* (1), 431-492.

21. Torrie, G. M.; Valleau, J. P., Monte Carlo free energy estimates using non-Boltzmann sampling: Application to the sub-critical Lennard-Jones fluid. *Chemical Physics Letters* **1974,** *28* (4), 578-581.

22. Kumar, S.; Rosenberg, J. M.; Bouzida, D.; Swendsen, R. H.; Kollman, P. A., THE weighted histogram analysis method for free-energy calculations on biomolecules. I. The method. *Journal of computational chemistry* **1992,** *13* (8), 1011-1021.

23. Souaille, M.; Roux, B. t., Extension to the weighted histogram analysis method: combining umbrella sampling with free energy calculations. *Computer Physics Communications* **2001,** *135* (1), 40-57.

24. Kästner, J.; Thiel, W., Bridging the gap between thermodynamic integration and umbrella sampling provides a novel analysis method: “Umbrella integration”. *The Journal of Chemical Physics* **2005,** *123* (14), 144104.

25. Park, S.; Schulten, K., Calculating potentials of mean force from steered molecular dynamics simulations. *J Chem Phys* **2004,** *120* (13), 5946-61.

26. Park, S.; Khalili-Araghi, F.; Tajkhorshid, E.; Schulten, K., Free energy calculation from steered molecular dynamics simulations using Jarzynski’s equality. *The Journal of Chemical Physics* **2003,** *119* (6), 3559-3566.

27. Darve, E.; Pohorille, A., Calculating free energies using average force. *The Journal of Chemical Physics* **2001,** *115* (20), 9169-9183.

28. Overton, E., *Vierteljahrsschr Naturforsch Ges Zurich* **1896,** *41*, 383.

29. Finkelstein, A., Water and nonelectrolyte permeability of lipid bilayer membranes. *The Journal of General Physiology* **1976,** *68* (2), 127-135.

30. Diamond, J. M.; Katz, Y., Interpretation of nonelectrolyte partition coefficients between dimyristoyl lecithin and water. *The Journal of Membrane Biology 17* (1), 121-154.

31. Marrink, S.-J.; Berendsen, H. J. C., Simulation of water transport through a lipid membrane. *The Journal of Physical Chemistry* **1994,** *98* (15), 4155-4168.

32. Parisio, G.; Stocchero, M.; Ferrarini, A., Passive Membrane Permeability: Beyond the Standard Solubility-Diffusion Model. *Journal of Chemical Theory and Computation* **2013,** *9* (12), 5236-5246.

33. Comer, J.; Schulten, K.; Chipot, C., Calculation of Lipid-Bilayer Permeabilities Using an Average Force. *Journal of Chemical Theory and Computation* **2014,** *10* (2), 554-564.

34. Comer, J.; Schulten, K.; Chipot, C., Diffusive Models of Membrane Permeation with Explicit Orientational Freedom. *Journal of Chemical Theory and Computation* **2014,** *10* (7), 2710-2718.

35. Riahi, S.; Rowley, C. N., Why Can Hydrogen Sulfide Permeate Cell Membranes? *Journal of the American Chemical Society* **2014,** *136* (43), 15111-15113.

36. Lamoureux, G.; Harder, E.; Vorobyov, I. V.; Roux, B.; MacKerell Jr, A. D., A polarizable model of water for molecular dynamics simulations of biomolecules. *Chemical Physics Letters* **2006,** *418* (1–3), 245-249.

37. Riahi, S.; Rowley, C. N., A Drude Polarizable Model for Liquid Hydrogen Sulfide. *The Journal of Physical Chemistry B* **2013,** *117* (17), 5222-5229.

38. Riahi, S.; Rowley, C. N., Solvation of Hydrogen Sulfide in Liquid Water and at the Water–Vapor Interface Using a Polarizable Force Field. *The Journal of Physical Chemistry B* **2014,** *118* (5), 1373-1380.

39. Chowdhary, J.; Harder, E.; Lopes, P. E. M.; Huang, L.; MacKerell, A. D.; Roux, B., A Polarizable Force Field of Dipalmitoylphosphatidylcholine Based on the Classical Drude Model for Molecular Dynamics Simulations of Lipids. *The Journal of Physical Chemistry B* **2013,** *117* (31), 9142-9160.

40. Terreno, E.; Sanino, A.; Carrera, C.; Castelli, D. D.; Giovenzana, G. B.; Lombardi, A.; Mazzon, R.; Milone, L.; Visigalli, M.; Aime, S., Determination of water permeability of paramagnetic liposomes of interest in MRI field. *Journal of Inorganic Biochemistry* **2008,** *102* (5–6), 1112-1119.

41. Bemporad, D.; Essex, J. W.; Luttmann, C., Permeation of Small Molecules through a Lipid Bilayer: A Computer Simulation Study. *The Journal of Physical Chemistry B* **2004,** *108* (15), 4875-4884.

42. Mathai, J. C.; Missner, A.; Kügler, P.; Saparov, S. M.; Zeidel, M. L.; Lee, J. K.; Pohl, P., No facilitator required for membrane transport of hydrogen sulfide. *Proceedings of the National Academy of Sciences* **2009,** *106* (39), 16633-16638.

43. Subczynski, W. K.; Hyde, J. S.; Kusumi, A., Oxygen permeability of phosphatidylcholine--cholesterol membranes. *Proceedings of the National Academy of Sciences of the United States of America* **1989,** *86* (12), 4474-8.

44. Beauchamp, R. O., Jr.; Bus, J. S.; Popp, J. A.; Boreiko, C. J.; Andjelkovich, D. A., A critical review of the literature on hydrogen sulfide toxicity. *Critical reviews in toxicology* **1984,** *13* (1), 25-97.

45. Orsi, M.; Essex, J. W., Permeability of drugs and hormones through a lipid bilayer: insights from dual-resolution molecular dynamics. *Soft Matter* **2010,** *6* (16), 3797-3808.

46. Paloncýová, M.; DeVane, R.; Murch, B.; Berka, K.; Otyepka, M., Amphiphilic Drug-Like Molecules Accumulate in a Membrane below the Head Group Region. *The Journal of Physical Chemistry B* **2014,** *118* (4), 1030-1039.

47. Wang, H. R., X.; Meng, F., Molecular dynamics simulation of six β-blocker drugs passing across POPC bilayer. *Molecular Simulation* **2016,** *42* (1), 56-63.

48. Kang, M.; Loverde, S. M., Molecular Simulation of the Concentration-Dependent Interaction of Hydrophobic Drugs with Model Cellular Membranes. *The Journal of Physical Chemistry B* **2014,** *118* (41), 11965-11972.

49. Ashrafuzzaman, M.; Tseng, C. Y.; Duszyk, M.; Tuszynski, J. A., Chemotherapy drugs form ion pores in membranes due to physical interactions with lipids. *Chemical biology & drug design* **2012,** *80* (6), 992-1002.

50. Notman, R.; Anwar, J., Breaching the skin barrier — Insights from molecular simulation of model membranes. *Advanced drug delivery reviews* **2013,** *65* (2), 237-250.

51. Anigbogu, A. N. C.; Williams, A. C.; Barry, B. W.; Edwards, H. G. M., Fourier transform raman spectroscopy of interactions between the penetration enhancer dimethyl sulfoxide and human stratum corneum. *International Journal of Pharmaceutics* **1995,** *125* (2), 265-282.

52. Williams, A. C.; Barry, B. W., Penetration enhancers. *Advanced drug delivery reviews* **2004,** *56* (5), 603-18.

53. Kumar, P.; Singh, S. K.; Mishra, D. N.; Girotra, P., Enhancement of ketorolac tromethamine permeability through rat skin using penetration enhancers: An ex-vivo study. *International Journal of Pharmaceutical Investigation* **2015,** *5* (3), 142-146.

54. Barry, B. W., Mode of action of penetration enhancers in human skin. *Journal of Controlled Release* **1987,** *6* (1), 85-97.

55. Notman, R.; Noro, M.; O'Malley, B.; Anwar, J., Molecular Basis for Dimethylsulfoxide (DMSO) Action on Lipid Membranes. *Journal of the American Chemical Society* **2006,** *128* (43), 13982-13983.

56. Gurtovenko, A. A.; Anwar, J., Modulating the structure and properties of cell membranes: the molecular mechanism of action of dimethyl sulfoxide. *The journal of physical chemistry. B* **2007,** *111* (35), 10453-60.

57. Hughes, Z. E.; Mark, A. E.; Mancera, R. L., Molecular Dynamics Simulations of the Interactions of DMSO with DPPC and DOPC Phospholipid Membranes. *The Journal of Physical Chemistry B* **2012,** *116* (39), 11911-11923.

58. Dabkowska, A. P.; Foglia, F.; Lawrence, M. J.; Lorenz, C. D.; McLain, S. E., On the solvation structure of dimethylsulfoxide/water around the phosphatidylcholine head group in solution. *The Journal of Chemical Physics* **2011,** *135* (22), 225105.

59. Gurtovenko, A. A.; Anwar, J., Interaction of Ethanol with Biological Membranes: The Formation of Non-bilayer Structures within the Membrane Interior and their Significance. *The Journal of Physical Chemistry B* **2009,** *113* (7), 1983-1992.

60. Posokhov, Y. O.; Kyrychenko, A., Effect of acetone accumulation on structure and dynamics of lipid membranes studied by molecular dynamics simulations. *Computational Biology and Chemistry* **2013,** *46*, 23-31.

61. Notman, R.; Noro, M. G.; Anwar, J., Interaction of Oleic Acid with Dipalmitoylphosphatidylcholine (DPPC) Bilayers Simulated by Molecular Dynamics. *The Journal of Physical Chemistry B* **2007,** *111* (44), 12748-12755.

62. John, N. W.; James, B., Voltage-Gated Sodium Channel Blockers; Target Validation and Therapeutic Potential. *Current Topics in Medicinal Chemistry* **2005,** *5* (6), 529-537.

63. Bagal, S. K.; Chapman, M. L.; Marron, B. E.; Prime, R.; Storer, R. I.; Swain, N. A., Recent progress in sodium channel modulators for pain. *Bioorganic & medicinal chemistry letters* **2014,** *24* (16), 3690-9.

64. Doyle, D. A.; Morais Cabral, J.; Pfuetzner, R. A.; Kuo, A.; Gulbis, J. M.; Cohen, S. L.; Chait, B. T.; MacKinnon, R., The structure of the potassium channel: molecular basis of K+ conduction and selectivity. *Science* **1998,** *280* (5360), 69-77.

65. Smart, O. S.; Goodfellow, J. M.; Wallace, B. A., The pore dimensions of gramicidin A. *Biophysical Journal* **1993,** *65* (6), 2455-2460.

66. Heginbotham, L.; Lu, Z.; Abramson, T.; MacKinnon, R., Mutations in the K+ channel signature sequence. *Biophysical journal* **1994,** *66* (4), 1061-1067.

67. Parsegian, A., Energy of an Ion crossing a Low Dielectric Membrane: Solutions to Four Relevant Electrostatic Problems. *Nature* **1969,** *221* (5183), 844-846.

68. Berneche, S.; Roux, B., Energetics of ion conduction through the K+ channel. *Nature* **2001,** *414* (6859), 73-7.

69. Noskov, S. Y.; Berneche, S.; Roux, B., Control of ion selectivity in potassium channels by electrostatic and dynamic properties of carbonyl ligands. *Nature* **2004,** *431* (7010), 830-834.

70. Aqvist, J.; Luzhkov, V., Ion permeation mechanism of the potassium channel. *Nature* **2000,** *404* (6780), 881-4.

71. Furini, S.; Domene, C., Atypical mechanism of conduction in potassium channels. *Proceedings of the National Academy of Sciences of the United States of America* **2009,** *106* (38), 16074-7.

72. Köpfer, D. A.; Song, C.; Gruene, T.; Sheldrick, G. M.; Zachariae, U.; de Groot, B. L., Ion permeation in K+ channels occurs by direct Coulomb knock-on. *Science* **2014,** *346* (6207), 352-355.

73. Jorgensen, C.; Darré, L.; Vanommeslaeghe, K.; Omoto, K.; Pryde, D.; Domene, C., In Silico Identification of PAP-1 Binding Sites in the Kv1.2 Potassium Channel. *Molecular Pharmaceutics* **2015,** *12* (4), 1299-1307.

74. Li, Y.; Barbault, F.; Delamar, M.; Zhang, R.; Hu, R., Targeted molecular dynamics (TMD) of the full-length KcsA potassium channel: on the role of the cytoplasmic domain in the opening process. *Journal of molecular modeling* **2013,** *19* (4), 1651-1666.

75. Monticelli, L.; Robertson, K. M.; MacCallum, J. L.; Tieleman, D. P., Computer simulation of the KvAP voltage-gated potassium channel: steered molecular dynamics of the voltage sensor. *FEBS Letters* **2004,** *564* (3), 325-332.

76. Roux, B., Ion Conduction and Selectivity in K+ Channels. *Annual Review of Biophysics and Biomolecular Structure* **2005,** *34* (1), 153-171.

77. Furini, S.; Domene, C., K(+) and Na(+) Conduction in Selective and Nonselective Ion Channels Via Molecular Dynamics Simulations. *Biophysical journal* **2013,** *105* (8), 1737-1745.

78. Payandeh, J.; Scheuer, T.; Zheng, N.; Catterall, W. A., The crystal structure of a voltage-gated sodium channel. *Nature* **2011,** *475* (7356), 353-8.

79. Payandeh, J.; Gamal El-Din, T. M.; Scheuer, T.; Zheng, N.; Catterall, W. A., Crystal structure of a voltage-gated sodium channel in two potentially inactivated states. *Nature* **2012,** *486* (7401), 135-139.

80. McCusker, E. C.; Bagneris, C.; Naylor, C. E.; Cole, A. R.; D'Avanzo, N.; Nichols, C. G.; Wallace, B. A., Structure of a bacterial voltage-gated sodium channel pore reveals mechanisms of opening and closing. *Nat Commun* **2012,** *3*, 1102.

81. Bagnéris, C.; DeCaen, P. G.; Hall, B. A.; Naylor, C. E.; Clapham, D. E.; Kay, C. W. M.; Wallace, B. A., Role of the C-terminal domain in the structure and function of tetrameric sodium channels. *Nat Commun* **2013,** *4*.

82. Shaya, D.; Findeisen, F.; Abderemane-Ali, F.; Arrigoni, C.; Wong, S.; Nurva, S. R.; Loussouarn, G.; Minor Jr, D. L., Structure of a Prokaryotic Sodium Channel Pore Reveals Essential Gating Elements and an Outer Ion Binding Site Common to Eukaryotic Channels. *Journal of molecular biology* **2014,** *426* (2), 467-483.

83. Carnevale, V.; Treptow, W.; Klein, M. L., Sodium Ion Binding Sites and Hydration in the Lumen of a Bacterial Ion Channel from Molecular Dynamics Simulations. *The Journal of Physical Chemistry Letters* **2011,** *2* (19), 2504-2508.

84. Corry, B.; Thomas, M., Mechanism of Ion Permeation and Selectivity in a Voltage Gated Sodium Channel. *J. Am. Chem. Soc.* **2012,** *134* (3), 1840-1846.

85. Furini, S.; Domene, C., On conduction in a bacterial sodium channel. *PLoS Comput Biol* **2012,** *8* (4), e1002476.

86. Qiu, H.; Shen, R.; Guo, W., Ion solvation and structural stability in a sodium channel investigated by molecular dynamics calculations. *Biochimica et biophysica acta* **2012,** *1818* (11), 2529-35.

87. Domene, C.; Klein, M. L.; Branduardi, D.; Gervasio, F. L.; Parrinello, M., Conformational changes and gating at the selectivity filter of potassium channels. *J Am Chem Soc* **2008,** *130* (29), 9474-80.

88. Zhou, Y.; Morais-Cabral, J. H.; Kaufman, A.; MacKinnon, R., Chemistry of ion coordination and hydration revealed by a K^+ channel-Fab complex at 2.0 Å resolution. *Nature* **2001,** *414*, 43-48.

89. Domene, C.; Furini, S., Dynamics, energetics, and selectivity of the low-K+ KcsA channel structure. *Journal of molecular biology* **2009,** *389* (3), 637-45.

90. Corry, B., Na(+)/Ca(2+) selectivity in the bacterial voltage-gated sodium channel NavAb. *PeerJ* **2013,** *1*, e16.

91. Benos, D. J.; Hyde, B. A.; Latorre, R., Sodium flux ratio through the amiloride-sensitive entry pathway in frog skin. *Journal of General Physiology* **1983,** *81* (5), 667-685.

92. Stock, L.; Delemotte, L.; Carnevale, V.; Treptow, W.; Klein, M. L., Conduction in a Biological Sodium Selective Channel. *The Journal of Physical Chemistry B* **2013,** *117* (14), 3782-3789.

93. Chakrabarti, N.; Ing, C.; Payandeh, J.; Zheng, N.; Catterall, W. A.; Pomès, R., Catalysis of Na+ permeation in the bacterial sodium channel NaVAb. *Proceedings of the National Academy of Sciences* **2013,** *110* (28), 11331-11336.

94. Domene, C.; Barbini, P.; Furini, S., Bias-Exchange Metadynamics Simulations: An Efficient Strategy for the Analysis of Conduction and Selectivity in Ion Channels. *J Chem Theory Comput* **2015,** *11* (4), 1896-906.

95. Boiteux, C.; Vorobyov, I.; Allen, T. W., Ion conduction and conformational flexibility of a bacterial voltage-gated sodium channel. *Proceedings of the National Academy of Sciences* **2014,** *111* (9), 3454-3459.

96. Ke, S.; Timin, E. N.; Stary-Weinzinger, A., Different inward and outward conduction mechanisms in NaVMs suggested by molecular dynamics simulations. *PLoS Comput Biol* **2014,** *10* (7), e1003746.

97. Furini, S.; Barbini, P.; Domene, C., Effects of the Protonation State of the EEEE Motif of a Bacterial Na(+)-channel on Conduction and Pore Structure. *Biophysical journal* **2014,** *106* (10), 2175-2183.

98. Ke, S.; Zangerl, E.-M.; Stary-Weinzinger, A., Distinct interactions of Na+ and Ca2+ ions with the selectivity filter of the bacterial sodium channel NaVAb. *Biochemical and Biophysical Research Communications* **2013,** *430* (4), 1272-1276.

99. Hille, B., Local anesthetics: hydrophilic and hydrophobic pathways for the drug-receptor reaction. *J Gen Physiol* **1977,** *69* (4), 497-515.

100. Raju, S. G.; Barber, A. F.; LeBard, D. N.; Klein, M. L.; Carnevale, V., Exploring Volatile General Anesthetic Binding to a Closed Membrane-Bound Bacterial Voltage-Gated Sodium Channel via Computation. *PLoS Computational Biology* **2013,** *9* (6), e1003090.

101. Kaczmarski, J. A.; Corry, B., Investigating the size and dynamics of voltage-gated sodium channel fenestrations: A molecular dynamics study. *Channels* **2014,** *8* (3), 264-277.

102. Nardi, A.; Damann, N.; Hertrampf, T.; Kless, A., Advances in targeting voltage-gated sodium channels with small molecules. *ChemMedChem* **2012,** *7* (10), 1712-40.

103. Martin, L. J.; Corry, B., Locating the Route of Entry and Binding Sites of Benzocaine and Phenytoin in a Bacterial Voltage Gated Sodium Channel. *PLoS Comput Biol* **2014,** *10* (7), e1003688.

104. Boiteux, C.; Vorobyov, I.; French, R. J.; French, C.; Yarov-Yarovoy, V.; Allen, T. W., Local anesthetic and antiepileptic drug access and binding to a bacterial voltage-gated sodium channel. *Proceedings of the National Academy of Sciences* **2014,** *111* (36), 13057-13062.

105. Jorgensen, C.; Darré, L.; Oakes, V.; Torella, R.; Pryde, D.; Domene, C., Lateral Fenestrations in K+-Channels Explored Using Molecular Dynamics Simulations. *Molecular Pharmaceutics* **2016,** *13* (7), 2263-2273.

106. Rudnick, G., Mechanisms of Biogenic Amine Neurotransmitter Transporters. In *Neurotransmitter Transporters: Structure, Function, and Regulation*, Reith, M. E. A., Ed. Humana Press: Totowa, NJ, 1997; pp 73-100.

107. Iversen, L., Neurotransmitter transporters and their impact on the development of psychopharmacology. *British journal of pharmacology* **2006,** *147 Suppl 1*, S82-8.

108. Amara, S. G.; Sonders, M. S., Neurotransmitter transporters as molecular targets for addictive drugs. *Drug and alcohol dependence* **1998,** *51* (1-2), 87-96.

109. Bisha, I.; Magistrato, A., The molecular mechanism of secondary sodium symporters elucidated through the lens of the computational microscope. *RSC Advances* **2016,** *6* (12), 9522-9540.

110. Yamashita, A.; Singh, S. K.; Kawate, T.; Jin, Y.; Gouaux, E., Crystal structure of a bacterial homologue of Na+/Cl--dependent neurotransmitter transporters. *Nature* **2005,** *437* (7056), 215-23.

111. Krishnamurthy, H.; Gouaux, E., X-ray structures of LeuT in substrate-free outward-open and apo inward-open states. *Nature* **2012,** *481* (7382), 469-74.

112. Singh, S. K.; Yamashita, A.; Gouaux, E., Antidepressant binding site in a bacterial homologue of neurotransmitter transporters. *Nature* **2007,** *448* (7156), 952-956.

113. Zhou, Z.; Zhen, J.; Karpowich, N. K.; Goetz, R. M.; Law, C. J.; Reith, M. E.; Wang, D. N., LeuT-desipramine structure reveals how antidepressants block neurotransmitter reuptake. *Science* **2007,** *317* (5843), 1390-3.

114. Malinauskaite, L.; Said, S.; Sahin, C.; Grouleff, J.; Shahsavar, A.; Bjerregaard, H.; Noer, P.; Severinsen, K.; Boesen, T.; Schiott, B.; Sinning, S.; Nissen, P., A conserved leucine occupies the empty substrate site of LeuT in the Na+-free return state. *Nat Commun* **2016,** *7*.

115. Celik, L.; Schiøtt, B.; Tajkhorshid, E., Substrate Binding and Formation of an Occluded State in the Leucine Transporter. *Biophysical journal* **2008,** *94* (5), 1600-1612.

116. Noskov, S. Y.; Roux, B., Control of ion selectivity in LeuT: two Na+ binding sites with two different mechanisms. *J Mol Biol* **2008,** *377* (3), 804-18.

117. Caplan, D. A.; Subbotina, J. O.; Noskov, S. Y., Molecular mechanism of ion-ion and ion-substrate coupling in the Na+-dependent leucine transporter LeuT. *Biophysical journal* **2008,** *95* (10), 4613-21.

118. Zhao, C.; Stolzenberg, S.; Gracia, L.; Weinstein, H.; Noskov, S.; Shi, L., Ion-controlled conformational dynamics in the outward-open transition from an occluded state of LeuT. *Biophysical journal* **2012,** *103* (5), 878-88.

119. Tavoulari, S.; Margheritis, E.; Nagarajan, A.; DeWitt, D. C.; Zhang, Y.-W.; Rosado, E.; Ravera, S.; Rhoades, E.; Forrest, L. R.; Rudnick, G., Two Na+ Sites Control Conformational Change in a Neurotransmitter Transporter Homolog. *Journal of Biological Chemistry* **2015**.

120. Zomot, E.; Bendahan, A.; Quick, M.; Zhao, Y.; Javitch, J. A.; Kanner, B. I., Mechanism of chloride interaction with neurotransmitter:sodium symporters. *Nature* **2007,** *449* (7163), 726-30.

121. Zomot, E.; Gur, M.; Bahar, I., Microseconds simulations reveal a new sodium-binding site and the mechanism of sodium-coupled substrate uptake by LeuT. *The Journal of biological chemistry* **2015,** *290* (1), 544-55.

122. Zhao, C.; Noskov, S. Y., The role of local hydration and hydrogen-bonding dynamics in ion and solute release from ion-coupled secondary transporters. *Biochemistry* **2011,** *50* (11), 1848-56.

123. Thomas, J. R.; Gedeon, P. C.; Grant, B. J.; Madura, J. D., LeuT conformational sampling utilizing accelerated molecular dynamics and principal component analysis. *Biophysical journal* **2012,** *103* (1), L1-3.

124. Cheng, M. H.; Bahar, I., Complete mapping of substrate translocation highlights the role of LeuT N-terminal segment in regulating transport cycle. *PLoS Comput Biol* **2014,** *10* (10), e1003879.

125. Gur, M.; Zomot, E.; Cheng, M. H.; Bahar, I., Energy landscape of LeuT from molecular simulations. *The Journal of Chemical Physics* **2015,** *143* (24), 243134.

126. Shaikh, S. A.; Tajkhorshid, E., Modeling and dynamics of the inward-facing state of a Na+/Cl- dependent neurotransmitter transporter homologue. *PLoS Comput Biol* **2010,** *6* (8).

127. Faham, S.; Watanabe, A.; Besserer, G. M.; Cascio, D.; Specht, A.; Hirayama, B. A.; Wright, E. M.; Abramson, J., The crystal structure of a sodium galactose transporter reveals mechanistic insights into Na+/sugar symport. *Science* **2008,** *321* (5890), 810-4.

128. Grouleff, J.; Sondergaard, S.; Koldso, H.; Schiott, B., Properties of an inward-facing state of LeuT: conformational stability and substrate release. *Biophysical journal* **2015,** *108* (6), 1390-9.

129. Chen, R.; Chung, S.-H., Molecular dynamics simulations of Na+ and leucine transport by LeuT. *Biochemical and Biophysical Research Communications* **2015,** *464* (1), 281-285.

130. Shi, L.; Quick, M.; Zhao, Y.; Weinstein, H.; Javitch, J. A., The mechanism of a neurotransmitter:sodium symporter--inward release of Na+ and substrate is triggered by substrate in a second binding site. *Molecular cell* **2008,** *30* (6), 667-77.

131. Quick, M.; Shi, L.; Zehnpfennig, B.; Weinstein, H.; Javitch, J. A., Experimental conditions can obscure the second high-affinity site in LeuT. *Nature structural & molecular biology* **2012,** *19* (2), 207-11.

132. Zhao, Y.; Terry, D. S.; Shi, L.; Quick, M.; Weinstein, H.; Blanchard, S. C.; Javitch, J. A., Substrate-modulated gating dynamics in a Na+-coupled neurotransmitter transporter homologue. *Nature* **2011,** *474* (7349), 109-113.

133. Singh, S. K.; Piscitelli, C. L.; Yamashita, A.; Gouaux, E., A competitive inhibitor traps LeuT in an open-to-out conformation. *Science* **2008,** *322* (5908), 1655-61.

134. Piscitelli, C. L.; Krishnamurthy, H.; Gouaux, E., Neurotransmitter/sodium symporter orthologue LeuT has a single high-affinity substrate site. *Nature* **2010,** *468* (7327), 1129-1132.

135. Wang, H.; Gouaux, E., Substrate binds in the S1 site of the F253A mutant of LeuT, a neurotransmitter sodium symporter homologue. *EMBO reports* **2012,** *13* (9), 861-6.

136. Wang, H.; Elferich, J.; Gouaux, E., Structures of LeuT in bicelles define conformation and substrate binding in a membrane-like context. *Nature structural & molecular biology* **2012,** *19* (2), 212-9.

137. Cheng, M. H.; Bahar, I., Coupled global and local changes direct substrate translocation by neurotransmitter-sodium symporter ortholog LeuT. *Biophysical journal* **2013,** *105* (3), 630-9.

138. Quick, M.; Winther, A. M.; Shi, L.; Nissen, P.; Weinstein, H.; Javitch, J. A., Binding of an octylglucoside detergent molecule in the second substrate (S2) site of LeuT establishes an inhibitor-bound conformation. *Proceedings of the National Academy of Sciences of the United States of America* **2009,** *106* (14), 5563-8.

139. Zhao, C.; Caplan, D. A.; Noskov, S. Y., Evaluations of the Absolute and Relative Free Energies for Antidepressant Binding to the Amino Acid Membrane Transporter LeuT with Free Energy Simulations. *Journal of Chemical Theory and Computation* **2010,** *6* (6), 1900-1914.

140. King, N.; Hittinger, C. T.; Carroll, S. B., Evolution of Key Cell Signaling and Adhesion Protein Families Predates Animal Origins. *Science* **2003,** *301* (5631), 361-363.

141. Jacobson, K. A., New paradigms in GPCR drug discovery. *Biochemical Pharmacology* **2015,** *98* (4), 541-555.

142. Lappano, R.; Maggiolini, M., G protein-coupled receptors: novel targets for drug discovery in cancer. *Nature reviews. Drug discovery* **2011,** *10* (1), 47-60.

143. Stevens, R. C.; Cherezov, V.; Katritch, V.; Abagyan, R.; Kuhn, P.; Rosen, H.; Wuthrich, K., The GPCR Network: a large-scale collaboration to determine human GPCR structure and function. *Nature reviews. Drug discovery* **2013,** *12* (1), 25-34.

144. Galandrin, S.; Bouvier, M., Distinct signaling profiles of beta1 and beta2 adrenergic receptor ligands toward adenylyl cyclase and mitogen-activated protein kinase reveals the pluridimensionality of efficacy. *Molecular pharmacology* **2006,** *70* (5), 1575-84.

145. Kobilka, B. K.; Deupi, X., Conformational complexity of G-protein-coupled receptors. *Trends in pharmacological sciences* **2007,** *28* (8), 397-406.

146. Rasmussen, S. G. F.; Choi, H.-J.; Rosenbaum, D. M.; Kobilka, T. S.; Thian, F. S.; Edwards, P. C.; Burghammer, M.; Ratnala, V. R. P.; Sanishvili, R.; Fischetti, R. F.; Schertler, G. F. X.; Weis, W. I.; Kobilka, B. K., Crystal structure of the human [bgr]2 adrenergic G-protein-coupled receptor. *Nature* **2007,** *450* (7168), 383-387.

147. Cherezov, V.; Rosenbaum, D. M.; Hanson, M. A.; Rasmussen, S. G. F.; Thian, F. S.; Kobilka, T. S.; Choi, H.-J.; Kuhn, P.; Weis, W. I.; Kobilka, B. K.; Stevens, R. C., High Resolution Crystal Structure of an Engineered Human β(2)-Adrenergic G protein-Coupled Receptor. *Science (New York, N.Y.)* **2007,** *318* (5854), 1258-1265.

148. Rosenbaum, D. M.; Cherezov, V.; Hanson, M. A.; Rasmussen, S. G. F.; Thian, F. S.; Kobilka, T. S.; Choi, H.-J.; Yao, X.-J.; Weis, W. I.; Stevens, R. C.; Kobilka, B. K., GPCR Engineering Yields High-Resolution Structural Insights into β2-Adrenergic Receptor Function. *Science* **2007,** *318* (5854), 1266-1273.

149. Hanson, M. A.; Cherezov, V.; Griffith, M. T.; Roth, C. B.; Jaakola, V.-P.; Chien, E. Y. T.; Velasquez, J.; Kuhn, P.; Stevens, R. C., A Specific Cholesterol Binding Site Is Established by the 2.8 Å Structure of the Human β₂-Adrenergic Receptor. *Structure 16* (6), 897-905.

150. Dror, R. O.; Arlow, D. H.; Borhani, D. W.; Jensen, M. Ø.; Piana, S.; Shaw, D. E., Identification of two distinct inactive conformations of the β2-adrenergic receptor reconciles structural and biochemical observations. *Proceedings of the National Academy of Sciences* **2009,** *106* (12), 4689-4694.

151. Ballesteros, J. A.; Jensen, A. D.; Liapakis, G.; Rasmussen, S. G.; Shi, L.; Gether, U.; Javitch, J. A., Activation of the beta 2-adrenergic receptor involves disruption of an ionic lock between the cytoplasmic ends of transmembrane segments 3 and 6. *The Journal of biological chemistry* **2001,** *276* (31), 29171-7.

152. Rosenbaum, D. M.; Zhang, C.; Lyons, J. A.; Holl, R.; Aragao, D.; Arlow, D. H.; Rasmussen, S. G. F.; Choi, H.-J.; DeVree, B. T.; Sunahara, R. K.; Chae, P. S.; Gellman, S. H.; Dror, R. O.; Shaw, D. E.; Weis, W. I.; Caffrey, M.; Gmeiner, P.; Kobilka, B. K., Structure and function of an irreversible agonist-[bgr]2 adrenoceptor complex. *Nature* **2011,** *469* (7329), 236-240.

153. Nygaard, R.; Zou, Y.; Dror, R. O.; Mildorf, T. J.; Arlow, D. H.; Manglik, A.; Pan, A. C.; Liu, C. W.; Fung, J. J.; Bokoch, M. P.; Thian, F. S.; Kobilka, T. S.; Shaw, D. E.; Mueller, L.; Prosser, R. S.; Kobilka, B. K., The dynamic process of beta(2)-adrenergic receptor activation. *Cell* **2013,** *152* (3), 532-42.

154. Dror, R. O.; Arlow, D. H.; Maragakis, P.; Mildorf, T. J.; Pan, A. C.; Xu, H.; Borhani, D. W.; Shaw, D. E., Activation mechanism of the beta2-adrenergic receptor. *Proceedings of the National Academy of Sciences of the United States of America* **2011,** *108* (46), 18684-9.

155. Botelho, A. V.; Huber, T.; Sakmar, T. P.; Brown, M. F., Curvature and hydrophobic forces drive oligomerization and modulate activity of rhodopsin in membranes. *Biophysical journal* **2006,** *91* (12), 4464-77.

156. Mondal, S.; Khelashvili, G.; Shan, J.; Andersen, O. S.; Weinstein, H., Quantitative modeling of membrane deformations by multihelical membrane proteins: application to G-protein coupled receptors. *Biophysical journal* **2011,** *101* (9), 2092-101.

157. Mondal, S.; Johnston, J. M.; Wang, H.; Khelashvili, G.; Filizola, M.; Weinstein, H., Membrane Driven Spatial Organization of GPCRs. *Scientific Reports* **2013,** *3*, 2909.

158. Calebiro, D.; Rieken, F.; Wagner, J.; Sungkaworn, T.; Zabel, U.; Borzi, A.; Cocucci, E.; Zürn, A.; Lohse, M. J., Single-molecule analysis of fluorescently labeled G-protein–coupled

receptors reveals complexes with distinct dynamics and organization. *Proceedings of the National Academy of Sciences* **2013,** *110* (2), 743-748.

159. Fung, J. J.; Deupi, X.; Pardo, L.; Yao, X. J.; Velez-Ruiz, G. A.; DeVree, B. T.; Sunahara, R. K.; Kobilka, B. K., Ligand-regulated oligomerization of β(2)-adrenoceptors in a model lipid bilayer. *The EMBO Journal* **2009,** *28* (21), 3315-3328.

160. Prasanna, X.; Chattopadhyay, A.; Sengupta, D., Cholesterol Modulates the Dimer Interface of the β₂-Adrenergic Receptor via Cholesterol Occupancy Sites. *Biophysical journal 106* (6), 1290-1300.

161. Neale, C.; Herce, Henry D.; Pomès, R.; García, Angel E., Can Specific Protein-Lipid Interactions Stabilize an Active State of the Beta 2 Adrenergic Receptor? *Biophysical journal 109* (8), 1652-1662.

162. Kalli, A. C.; Sansom, M. S. P.; Reithmeier, R. A. F., Molecular Dynamics Simulations of the Bacterial UraA H⁺-Uracil Symporter in Lipid Bilayers Reveal a Closed State and a Selective Interaction with Cardiolipin. *PLoS computational biology* **2015,** *11* (3), e1004123.

163. Horn, J. N.; Kao, T.-c.; Grossfield, A., Coarse-grained Molecular Dynamics Provides Insight into the Interactions of Lipids and Cholesterol with Rhodopsin. *Advances in experimental medicine and biology* **2014,** *796*, 75-94.

164. Sengupta, D.; Chattopadhyay, A., Molecular dynamics simulations of GPCR-cholesterol interaction: An emerging paradigm. *Biochimica et biophysica acta* **2015,** *1848* (9), 1775-82.

165. Prasanna, X.; Chattopadhyay, A.; Sengupta, D., Role of Lipid-Mediated Effects in β2-Adrenergic Receptor Dimerization. In *Biochemical Roles of Eukaryotic Cell Surface Macromolecules*, Chakrabarti, A.; Surolia, A., Eds. Springer International Publishing: Cham, 2015; pp 247-261.